Electronic Supplementary Information

Colloidal silica assisted fabrication of N, O, S-tridoped porous carbon nanosheets with excellent oxygen reduction performance

Zihao Xing,[a] Meiling Xiao,[b] Zilong Guo[a] and Wensheng Yang*[a]

[a]State Key Laboratory of Inorganic Synthesis and Preparative Chemistry, College of Chemistry, Jilin University, Changchun 130012, P. R. China

[b]Department of Chemical Engineering, Waterloo Institute for Nanotechnology, University of Waterloo, 200 University Avenue West, Waterloo, Ontario N2L3G1, Canada

Experiment Section

Chemicals

1,8-diaminonaphthalene (DAN) and ammonium peroxydisulphate ($(NH_4)_2S_2O_8$) were purchased from Aladdin Company. Colloidal silica dispersion (Ludox ® HS-40, 40 wt.% suspension in water, particle size≈12 nm) was purchased from Sigma-Aldrich. 5 wt.% Nafion ionomer was obtained from Aldrich. Perchloric acid was purchased from Alfa Aesar. Commercial state-of-the-art 20 wt% Pt/C (Johnson Matthey Company, HiSPEC™ 3000) was used as the benchmark for comparison and was denoted as Pt/C. Hydrofluoric acid (≥40%) and were purchased from the Beijing Chemical Factory (Beijing, China) and ethanol were from the Shanghai Chemical Factory (Shanghai, China) and used as received without further purification. Ultrapure water (Millipore, 18.2 MΩ·cm) was used throughout all the experiments.

Materials synthesis

In a typical procedure, 200 mg 1,8-diaminonaphthalene (DAN) monomer was firstly dissolved in 50 mL ethanol under continuous stirring at room temperature and then mixed with certain amount of colloidal silica dispersion (0, 0.5, 1.0 and 2.0 g). Then 576 mg $(NH_4)_2S_2O_8$ oxidant was added with vigorous stirring. The polymerization was conducted for 24 h. After drying the mixture by using a rotary evaporator, the obtained PDAN/silica composites were pyrolyzed under flowing N_2 at 900℃ for 3h. The SiO_2 particles were etched out finally by HF solution to obtain the porous N, O, S-tridoped carbon nanosheets.

Electrochemical Measurements

RRDE measurements were conducted by liner sweep voltammetry (LSV) from 1.1 V to 0.2 V at a scan rate of 5 mV s^{-1} at 1600 rpm, while the ring electrode was held at 1.3 V vs. RHE. All the ORR currents presented in the figures are Faradaic currents, i.e. after correction for the capacitive current. The following equations were used to calculate n (the apparent number of electrons transferred during ORR) and % H_2O_2 (the percentage of H_2O_2 released during ORR).

$$n = \frac{4I_D}{I_D + (I_R/N)} \qquad (1)$$

$$\%H_2O_2 = 100\,\frac{2I_R/N}{I_D + (I_R/N)} \qquad (2)$$

Where I_D is the Faradaic current at the disk, I_R the Faradaic current at the ring and N is the H_2O_2 collection coefficient at the ring. The kinetic current (I_k) can be calculated by

the Koutechy-Levich equation given blow:

$$\frac{1}{I}=\frac{1}{I_L}+\frac{1}{I_K} \qquad (3)$$

The I_L term can be obtained from the Levich equation:

$$I_L = 0.62nAFC_0(D_0)^{2/3}\nu^{-\frac{1}{6}} \qquad (4)$$

where n is the number of electrons transferred; F is Faraday's constant(96,485 C mol^{-1}); A is the area of the electrode (0:196 cm^2); D is the diffusion coefficient of O_2 in 0.1 M KOH solution (1.9×10^{-5} cm^2 s^{-1}); $\nu$is the kinematic viscosity of the electrolyte (1.01×10^{-2} cm^2 s^{-1}); ω is the angular frequency of rotation, ω = 2πf/60, f is the RDE rotation rate in rpm, and C_0 is the concentration of molecular oxygen in 0.1M KOH solution(1.26×10^{-6} mol cm^{-3}). In all figures, the potentials were converted to values versus the reversible hydrogen electrode (RHE). The conversion from SCE to RHE is done by measuring the voltage ΔE between the SCE and a Pt-black coated Pt wire immersed in the same electrolyte saturated with H_2. The measured ΔE was 0.998 V. All experiments were carried out at about 25°C.

Characterizations

Scanning electron microscopy (SEM) measurements were performed with an XL 30 ESEM FEG field emission scanning electron microscope. Transmission electron microscopy (TEM), high-annular dark-field scanning transmission electron microscopy (STEM) and element mapping analysis were conducted on Philips TECNAI G2 electron microscope operating at 200 kV. Raman spectra were collected on a J-Y T64000 Raman spectrometer with 514.5 nm wavelength incident laser light. The

textural and morphological features of the various carbon supports and catalysts prepared were determined by nitrogen physisorption at 77 K in a Micromeritics ASAP 2020. Textural properties such as the specific surface area, pore volume and pore size distribution were calculated from each corresponding nitrogen adsorption−desorption isotherm, applying the Brunauer−Emmett−Teller (BET) equation and the Barrett−Joyner−Halenda (BJH). X-ray photoelectron spectroscopy (XPS) measurements were carried out on Mg K_{α} radiation source (Kratos XSAM-800 spectrometer). The bulk compositions were evaluated by inductively coupled plasma optical emission spectrometer (X Series 2, Thermo Scientific USA).

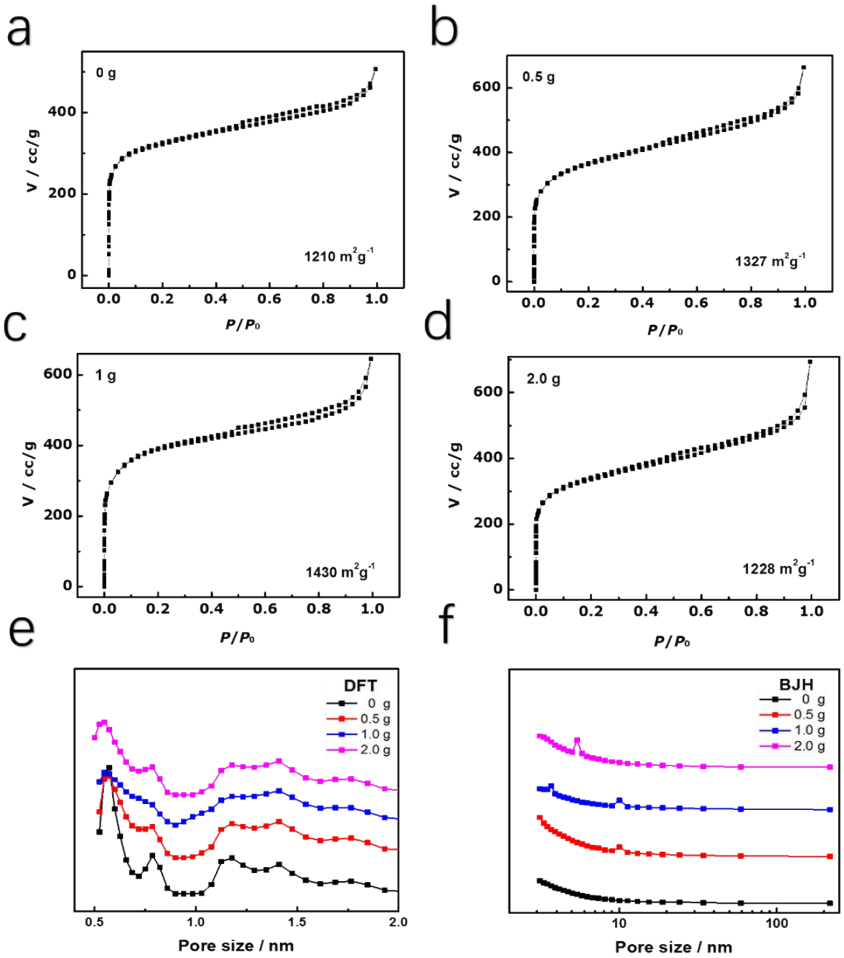

Fig. S1. Nitrogen adsorption-desorption isotherms of the N, O, S-tridoped carbon nanosheets fabricated with the assistance of (a) 0, (b) 0.5, (c) 1.0 and (d) 2.0 g colloidal silica. Surface areas of the nanosheets were determined to be 1210, 1327, 1430 and 1228 m^2 g^{-1} when the amount of silica used were 0, 0.5, 1.0 and 2.0 g. By utilizing the nonlocal density functional theory (NLDFT, in the range up to 2 nm) and Barrett-Joyner-Halenda (BJH, in the range of 2–100 nm) method, the derived pore size distribution plots indicate that only mesopores (<2 nm) were identified for the nanosheets fabricated without the silica and both micropores and mesopores centered around 10 nm were identifiable for the nanosheets fabricated with assistance of 0.5 and 1.0 g silica. The mesopore size was smaller than that of the silica template (12 nm), attributed to the shrinking of the silica during the pyrolysis reaction.[1] In presence of 2.0

g silica, the mesopores decreased to 6 nm, attributed to aggregation of the silica template.[2] Correspondingly, the surface area decreased from 1430 to 1228 m^2 g^{-1} when the amount of silica increased from 1.0 to 2.0 g.

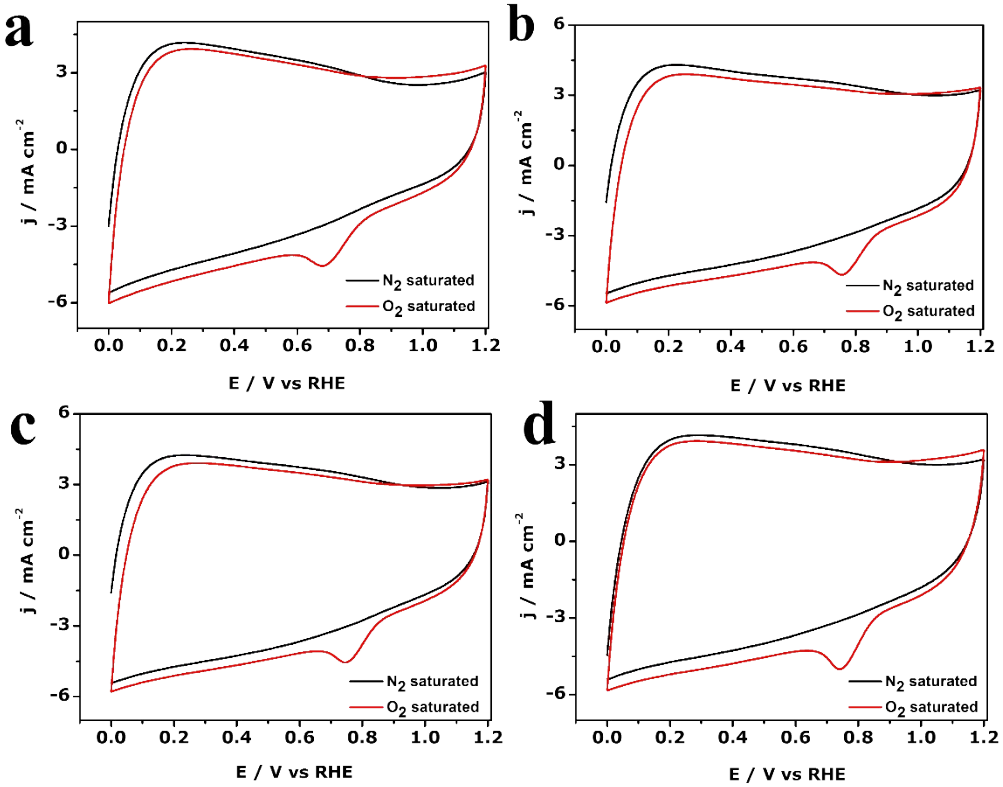

Fig. S2. CVs of the tridoped catalysts fabricated with the assistance of (a) 0, (b) 0.5, (c) 1.0 and (d) 2.0 g colloidal silica in N_2- (black) and O_2- (red) saturated 0.1 M KOH solution. The data were collected with potential scanned between 0 and 1.2 V at a scan rate of 20 mV/s.

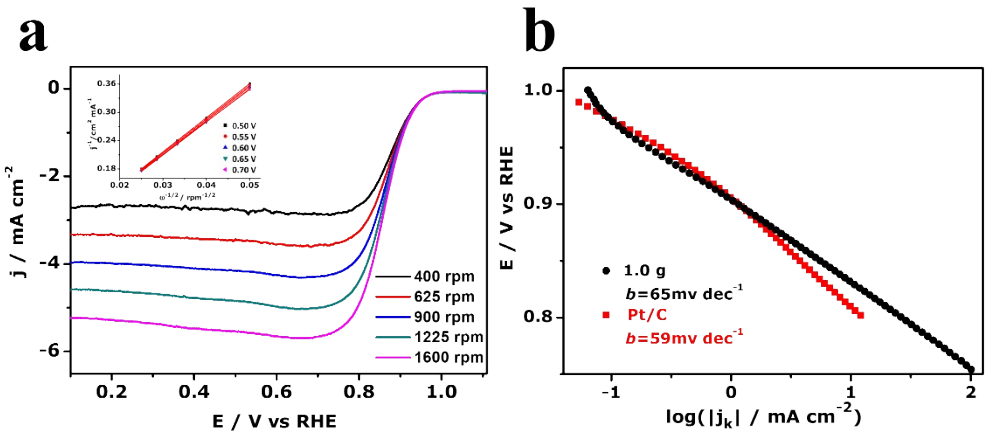

Fig. S3. (a) Liner sweep voltammetry (LSV) for oxygen reduction on the tridoped catalyst fabricated with 1.0 g silica in O_2-saturated 0.1 M KOH solution at rotation speeds of 400, 625, 900, 1225, and 1600 rpm with a fixed scan rate of 5 mV s^{-1} in the RDE measurements. Insert gives the corresponding Koutecky-Levich (K-L) plots derived from the LSV results, from which charge transfer numbers were calculated to be in the range of 3.90 to 4.05. (b) Tafel slopes for the tridoped catalyst fabricated with 1.0 g silica and the commercial Pt/C catalyst. Both the catalysts present slopes around 60 mV dec^{-1}, suggesting the first electron transfer is the rate-determining step in the ORR process for both the catalysts.

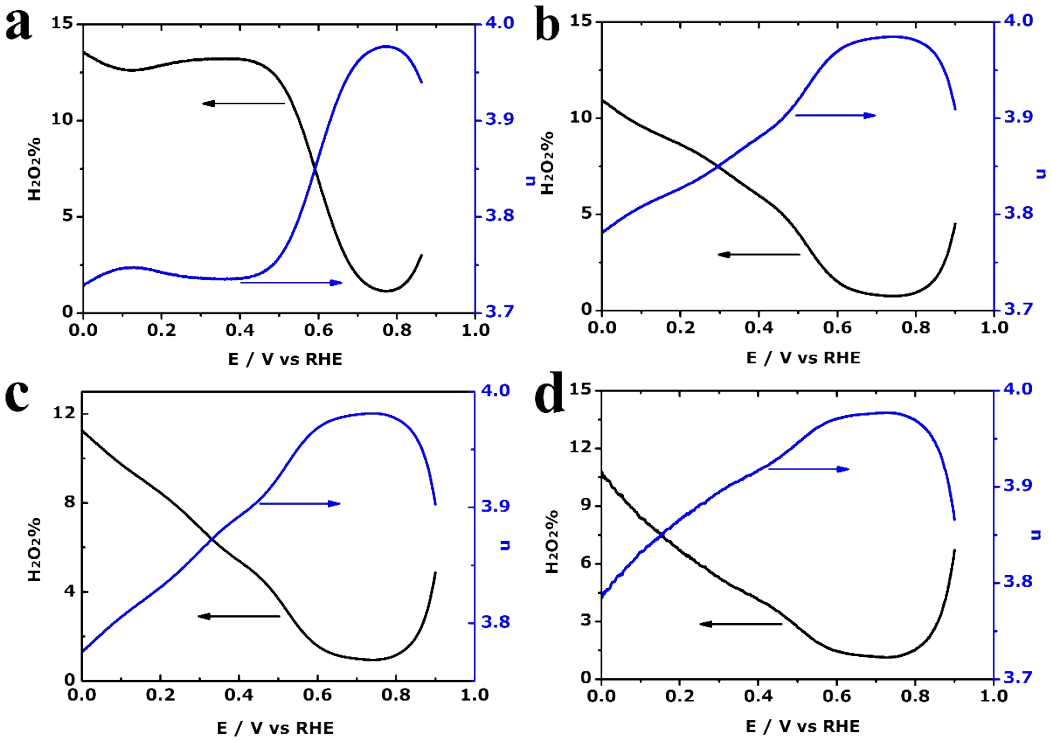

Fig. S4. The H_2O_2 yielding and corresponding electron transfer number calculated using RRDE method for the tridoped catalysts fabricated with the assistance of (a) 0, (b) 0.5, (c) 1.0 and (d) 2.0 g silica. The H_2O_2 production ratio for the catalyst fabricated without silica was in the range from 1.3% to 13.2%, with charge transfer numbers of 3.72–3.97. For the catalysts fabricated with 0.5, 1.0 and 2.0 g silica, the yields of H_2O_2 were in the range from 0.5% to 12%, with charge transfer numbers of 3.78–3.99.

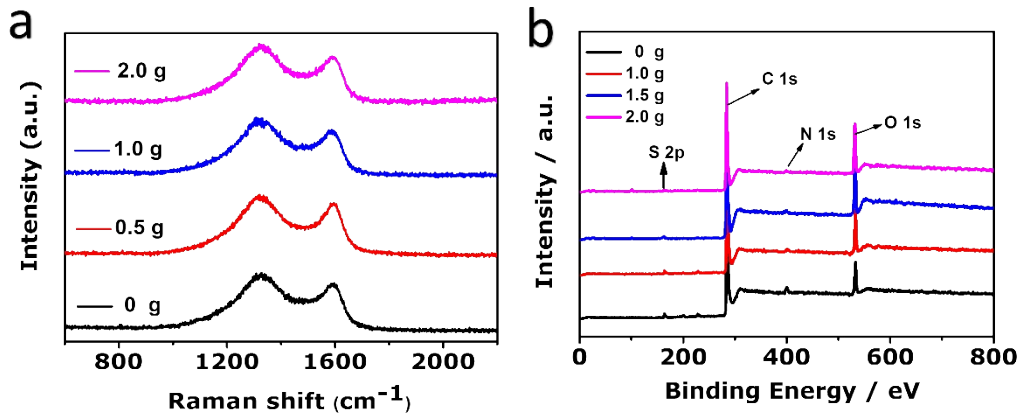

Fig. S5. (a) Raman spectra of different catalysts fabricated with 0, 0.5, 1.0 and 2.0 g silica. Intensity ratio of the D and G bands at 1360 and 1586 cm^{-1} increased from 1.71 to 1.78, 1.86 and 1.97, with the amount of colloidal silica used increased from 0 to 0.5, 1.0 and 2.0 g, indicating the increased defective sites in the catalysts with the increased amount of the silica; (b) The XPS survey spectra of catalysts fabricated with 1.0 g silica in the region of 0-1200 eV. The peaks of N, O, S and C were identifiable in the spectra.

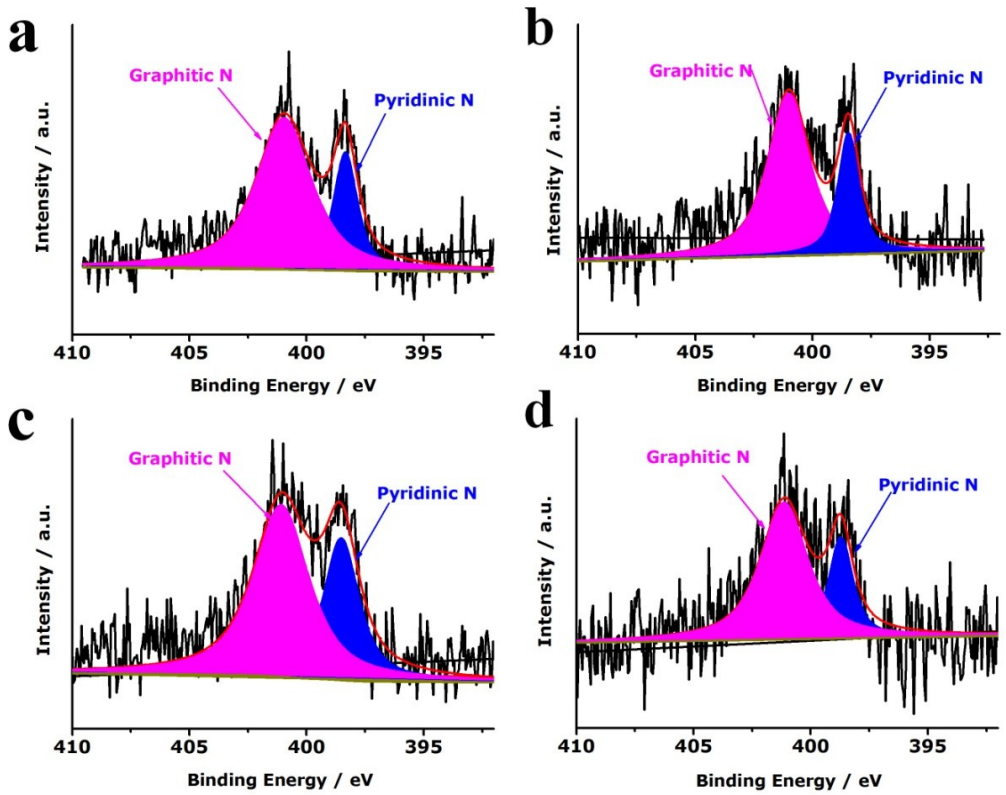

Fig. S6. High resolution XPS spectra of N 1s for the N, O, S-tridoped carbon nanosheets fabricated with the assistance of (a) 0, (b) 0.5, (c) 1.0 and (d) 2.0 g colloidal silica. The N 1s peak in the spectra was further deconvoluted into two peaks corresponding to pyridinic N (398.4 eV) and graphitic N (401.0 eV). No pyrrolic N (399.3 eV) was identified due to the high temperature (900 ^{o}C) used, which promoted the transformation of less stable pyrrolic N into more stable pyridinic and/or graphite N.[3,4]

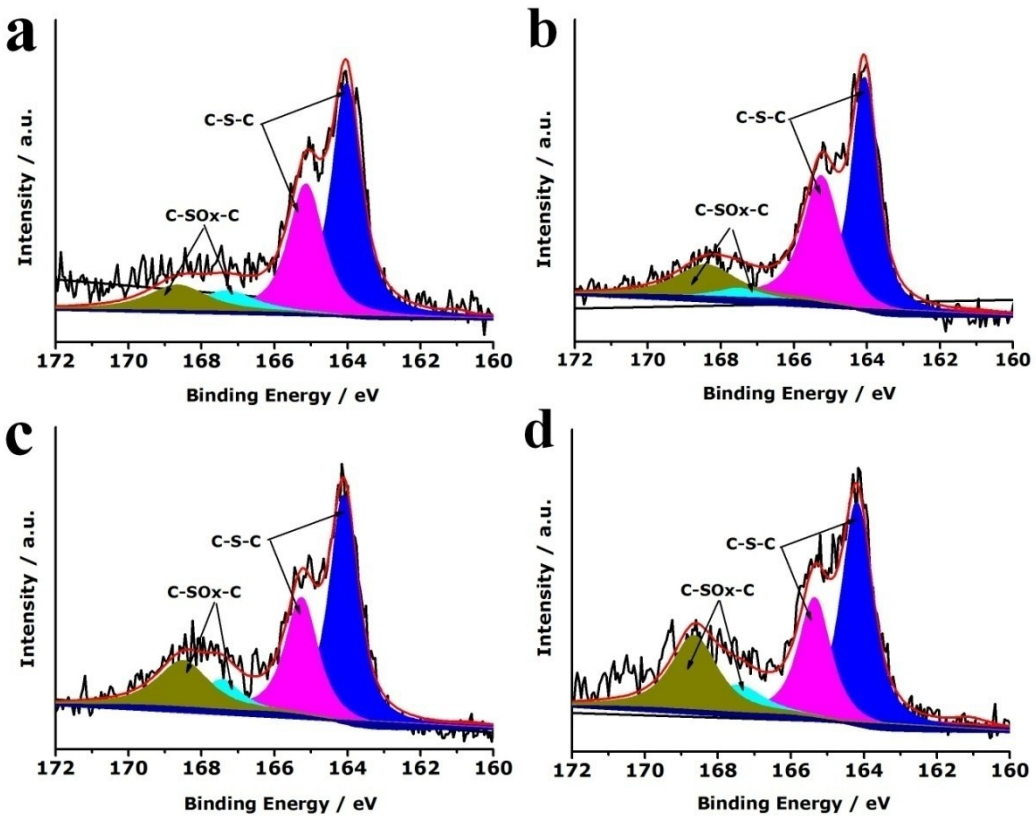

Fig. S7. High resolution XPS spectra of S 2p for the N, O, S-tridoped carbon nanosheets fabricated with the assistance of (a) 0, (b) 0.5, (c) 1.0 and (d) 2.0 g colloidal silica. The S 2p peak was deconvoluted into two main peaks associated with C-S-C (163.8/165.1 eV) and C-SOx-C (167.3/168.6 eV) species.

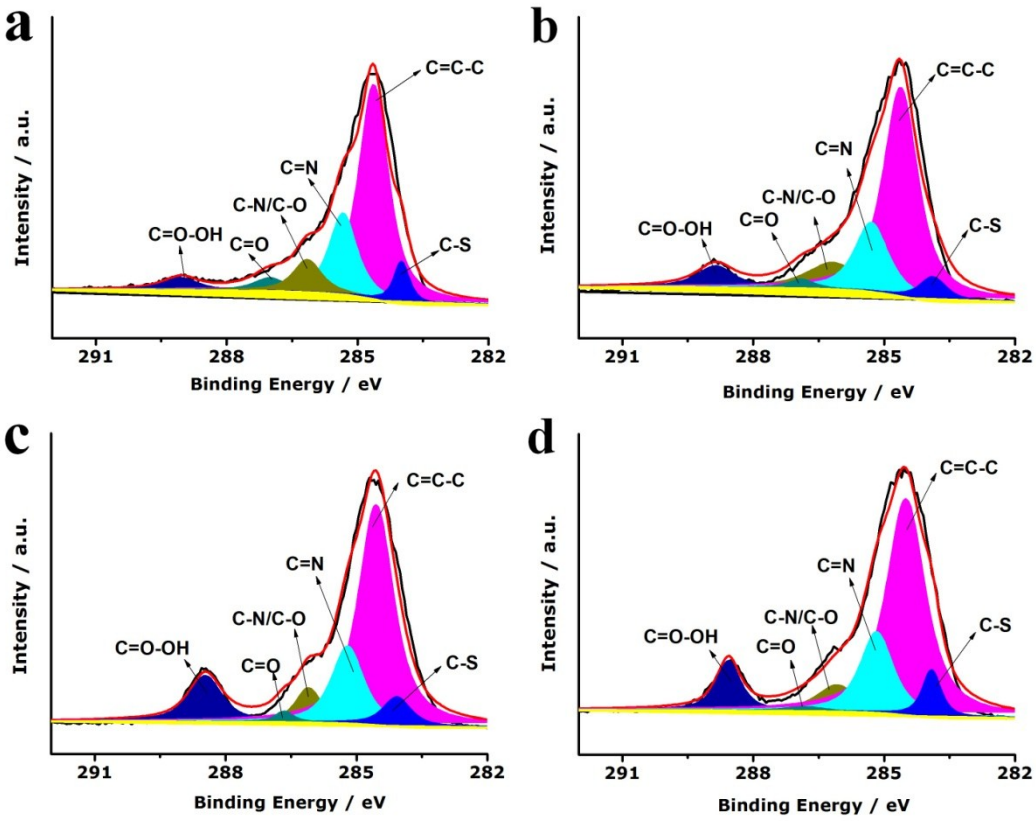

Fig. S8. High resolution XPS spectra of C 1s for the N, O, S-tridoped carbon nanosheets fabricated with the assistance of (a) 0, (b) 0.5, (c) 1.0 and (d) 2.0 g colloidal silica. The C 1s peaks corresponded to C-S (283.9 eV), C=C (284.6 eV), C=N (285.3 eV), C-O/C-N (286.1 eV), C=O (286.9 eV) and C=O-OH (288.6 eV) moieties were observable, which further proved the successful incorporation of N (C=N) and S (C-S) as well as into O (C=O, C=O-OH) into the carbons.

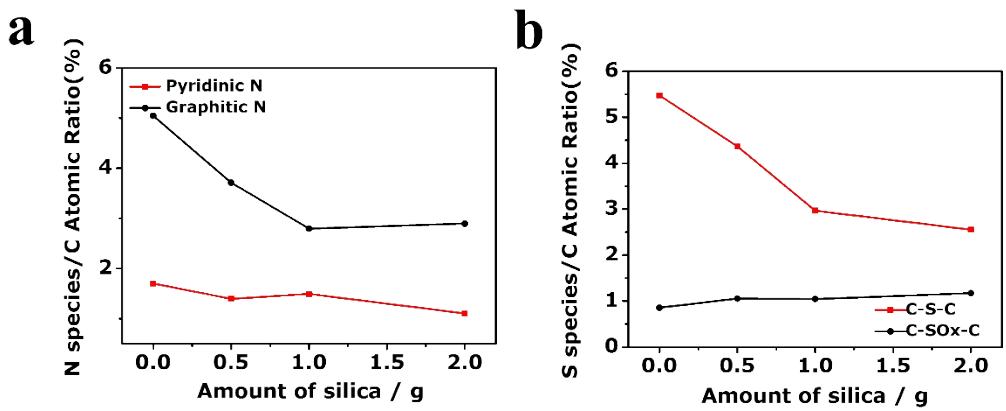

Fig. S9. Variations of the atomic ratios of (a) N/C and (b) S/C with the amount of colloidal silica used in the reactions. The ratios of N(graphite)/C were 5.0%, 3.7%, 2.8% and 2.9%, and these of N(pyridinic)/C were 1.7%, 1.4%, 1.5% and 1.1%, respectively, when the amounts of silica used were 0, 0.5, 1.0 and 2.0 g. The ratios of S(C-S-C)/C were 5.5%, 4.4%, 3.0% and 2.6%, and these of S(C-SO_X-C)/C were 0.8%, 1.1%, 1.0% and 1.2%, respectively, when the amounts of silica used were 0, 0.5, 1.0 and 2.0 g.

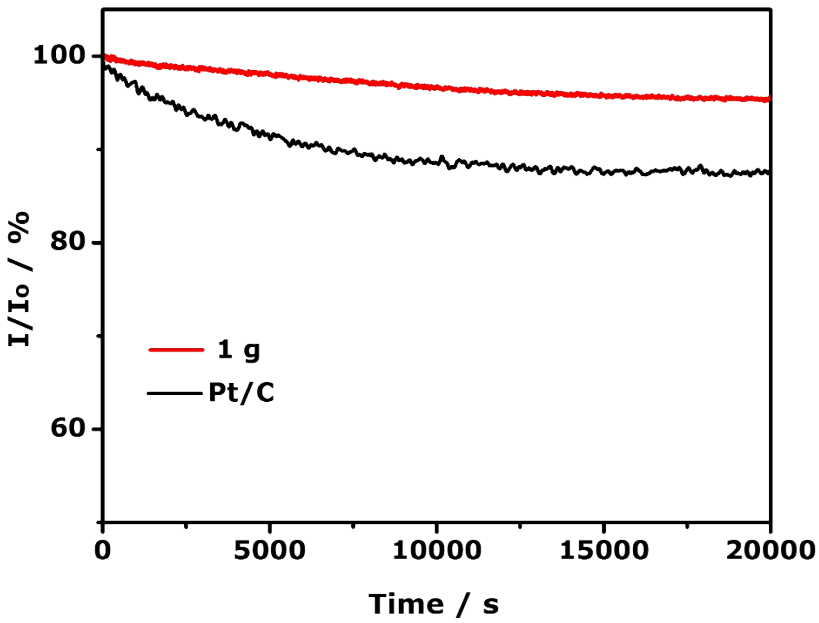

Fig. S10 Chronoamperometric curves for the N, O, S-tridoped carbon nanosheets fabricated with the assistance of 1.0 g silica (red curve) and commercial Pt/C (black curve) in O_2-saturated 0.1 KOH at constant potential of 0.8 V at 1600 rpm. The commercial Pt/C exhibited a loss of 10% in the activity after 20000 s, while the nanosheets showed only a loss of 4% in the of activity over the same period, indicating the excellent stability of the tridoped nanosheets in the ORR process.

Table S1. Comparison of ORR activity of the N,O,S-tridoped carbon nanosheets fabricated with the assistance of 1.0 g colloidal silica with the reported heteroatoms-doped carbon-based materials in 0.1 M KOH electrolyte.

Catalyst	Onset potential (V)	Half-wave potential (V)	Reference in main text
N,O,S-tridoped carbon nanosheets	**1.02**	**0.86**	**This work**
Commercial Pt/C	1.04	0.84	--
Mesoporous N-doped carbon nanosheets	0.91	0.81	8
Eggplant-derived microporous carbon sheets	0.86	--	9
N-doped food-grade-derived 3D mesoporous carbon foams	0.97	0.83	10
Polyaniline-derived N,O-codoped carbons	0.94	--	11
Carbon nanofiber@N-doped graphene blends	0.93	0.80	12
N,O,S-tridoped polypyrrole derived nanoporous carbons	0.96	0.74	24

References

1. Y. Ono, K. Nakashima, M. Sano, Y. Kanekiyo, K. Inoue, J. Hojo and S. Shinakai, *Chem. Commun.*, 1998, **14**, 1477–1478.

2. S. Han, A. K. Sohn and T. Hyeon, *Chem. Mater.*, 2000, **12**, 3337–3341.

3. G. Liu, X. G. Li, J. W. Lee and B. N. Popov, *Catal. Sci. Technol.*, 2011, **1**, 207–217.

4. R. Ning, C. J. Ge, Q. Liu, J. Q. Tian, A. M. Asiri, K. A. Alamry, C. M. Liu and X. P. Sun, *Carbon*, 2014, **78**, 60-69.